

Hybrid superconductor–quantum dot devices

Silvano De Franceschi^{1*}, Leo Kouwenhoven², Christian Schönberger³ and Wolfgang Wernsdorfer⁴

Advances in nanofabrication techniques have made it possible to make devices in which superconducting electrodes are connected to non-superconducting nanostructures such as quantum dots. The properties of these hybrid devices result from a combination of a macroscopic quantum phenomenon involving large numbers of electrons (superconductivity) and the ability to control single electrons, offered by quantum dots. Here we review research into electron transport and other fundamental processes that have been studied in these devices. We also describe potential applications, such as a transistor in which the direction of a supercurrent can be reversed by adding just one electron to a quantum dot.

In a superconductor, a significant fraction of the free electrons occupy the same quantum state at temperatures below the superconducting transition temperature, and the collective motion of the electrons in this state leads to a flow of charge without any dissipation or resistance¹. This state, which is called a condensate, is protected from other (dissipative) states by an energy gap. Note that the condensate in even an extremely small superconducting sample (volume $\sim \mu\text{m}^3$) contains millions of electrons — superconductivity is a truly macroscopic phenomenon.

The electrons in metals and semiconductors behave very differently to those in superconductors. For example, it is possible to trap small numbers of electrons in submicrometre-sized boxes known as quantum dots^{2,3}, and to add or remove single electrons by applying voltages to gate electrodes. This approach is now routinely used to control the number of electrons (and hence the spin) on semiconductor quantum dots, carbon nanotubes and various small molecules.

This Review describes the new physics and device possibilities that are opened when superconductors (in which large numbers of electrons are free to move) are connected to quantum dots (which can be used to trap single electrons). In particular we will focus on devices in which two superconducting electrodes are connected to a single quantum dot.

Such devices are similar to Josephson junctions⁴, which are an important building block in devices such as superconducting quantum interference devices (SQUIDS)⁵ and superconducting quantum bits (qubits)⁶. Josephson junctions are often made by sandwiching an insulator between two superconducting leads, but they can also be made by replacing the insulator with a nanoscale superconducting bridge or a metal in the normal (ie, non-superconducting) state⁷. The superconducting state 'leaks' across the junction, resulting in a quantum coherent coupling between the two superconductors that depends on the properties of the material in the region between them. As we shall discuss, by controlling the degrees of freedom of a quantum dot between two superconducting electrodes, it is possible to explore a wide range of physical phenomena including electron transport, Kondo physics, quantum entanglement and new types of fundamental particles.

Basic concepts

Figure 1 shows three examples of quantum dot junctions between superconductors. Figure 1a shows a device in which breaks in a ring of Ti/Al (which superconducts at low temperatures) are bridged by InAs nanowires⁸, and the strength of the coupling can be tuned by gate electrodes that cross the nanowires. In Figure 1b a nanoscale island of

SiGe forms the junction between two (much larger) Al superconducting electrodes⁹. Figure 1c shows the smallest such junction observed so far — in this example a single C_{60} molecule has been placed in a notch that has been created in an Al superconducting wire¹⁰.

Despite their differences, these three devices can all be modelled as two superconductors separated by a gate-controlled quantum dot that has distinct energy levels for electrons (or holes; Fig. 2). Here, the highest occupied state has an energy that is ϵ_0 below the Fermi energy of the superconductors. The energy levels also have a width Γ that corresponds to their finite lifetime (which is caused by electrons tunnelling out of the levels). When an extra electron is added to the dot it occupies an orbital with an energy that is $U + \Delta\epsilon$ higher than the previous highest level, where U is the charging energy needed to overcome the increased Coulomb repulsion³ between the electrons, and $\Delta\epsilon$ is the spacing between successive energy levels in the quantum dot. The superconducting condensates are at the Fermi energy, protected from the occupied quasiparticle states below and the empty states above by energy gaps of Δ . The quasiparticles are like electrons and have the same elementary charge, e . The basic element in the superconducting condensate, on the other hand, is a pair of electrons, also known as a Cooper pair¹.

To establish an electric current in a hybrid device, the singly charged quasiparticles and/or the doubly charged Cooper pairs have to tunnel from one electrode to the quantum dot and then from the quantum dot to the other electrode. An important concept in experiments with quantum dots is the Coulomb blockade: basically, a current will only flow through a quantum dot when the incoming electrons have enough energy to overcome the Coulomb repulsion due to the electrons that are already on the dot. The energy barrier caused by Coulomb repulsion can be lowered with the aid of a gate voltage, acting on ϵ_0 , or a sufficiently large source–drain bias voltage. When the current through the dot (or the differential conductance of the dot) is plotted against the gate voltage on one axis and the source–drain bias voltage on another axis, the Coulomb blockade manifests itself as a series of diamonds inside which current cannot flow, separated by regions of voltage space in which current does flow.

We can distinguish three different regimes, depending on the relative values of the width of the levels, Γ , the superconducting gap, Δ , and the charging energy, U . When Γ is the largest energy scale, the Cooper pairs can resonantly tunnel across the quantum dot, so supercurrent transport takes place in this strong-coupling regime (Fig. 2c).

When Γ is very small, the charging energy is too high for the Cooper pairs to tunnel across the dot (because they have charge

¹SPSMS/LaTEQS, CEA-INAC/UJF-Grenoble 1, 17 Rue des Martyrs, 38054 Grenoble Cedex 9, France, ²Kavli Institute of NanoScience, Delft University of Technology, PO Box 5046, 2600 GA, Delft, the Netherlands, ³Department of Physics, University of Basel, Klingelbergstr. 82, CH-4056 Basel, Switzerland, ⁴Institut Néel, associé à l'UJF, CNRS, BP 166, 38042 Grenoble Cedex 9, France. *e-mail: silvano.defranceschi@cea.fr

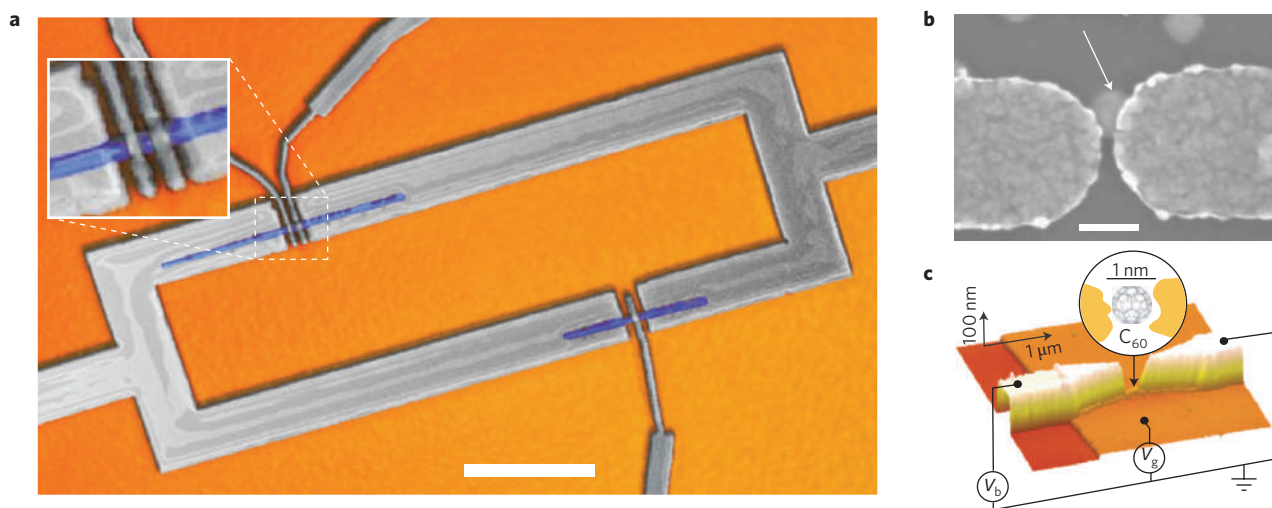


Figure 1 | Three hybrid superconductor–quantum dot devices. **a**, Scanning electron microscope (SEM) image of a SQUID device made of Ti/Al (grey), which becomes superconducting below ~ 1 K. Each arm of the superconducting ring contains a break that is bridged by an InAs nanowire (blue). A pair of Al gates (~ 65 nm apart) is used to define a quantum dot in one of the nanowires (top left and inset) by creating tunable tunnel barriers in the nanowire. The coupling between the superconducting leads on either side of the quantum dot is determined by the electronic characteristics of the dot. The other nanowire (bottom right) forms a simpler superconducting weak link, with just one gate to control the strength of the Josephson coupling. Scale bar: 2 μ m. **b**, SEM image of a self-assembled SiGe quantum dot (indicated by an arrow) connected to two Al electrodes. The number of carriers (holes) confined on the quantum dot can be controlled with a back gate buried in the substrate. Scale bar: 100 nm. **c**, Atomic force microscope (AFM) image of an Al break junction containing a notch that is filled by a single C_{60} molecule (see schematic inset). The junction, which is formed by an electromigration process, rests on top of an oxidized Al electrode that is used as a back gate. This gate can tune the electronic state of the molecule between two charge states that differ by one electron. V_b and V_g are the applied source–drain bias and gate voltage, respectively. Figures reproduced from: **b**, ref. 9, © 2010 NPG; **c**, ref. 85, © 2008 NPG.

2e), so there is no supercurrent. Quasiparticle tunnelling is therefore the dominant transport mechanism in the weak-coupling regime (Fig. 2d).

When Γ , Δ and U are comparable to each other, as they are in the intermediate-coupling regime, the situation is more complex (Fig. 2e). Cooper pairs can split into quasiparticles with charge $1e$ that are able to tunnel individually across the quantum dot because the Coulomb-energy cost for particles with charge $1e$ is lower than for particles with charge $2e$. If the time it takes the quasiparticles to tunnel across the dot ($\sim h/\Gamma$, where h is Planck's constant) is shorter than the characteristic coherence time of the Cooper pairs ($\sim h/\Delta$), it is possible for the Cooper pairs to reform in the second electrode. This condition ($\Delta < \Gamma$) is not satisfied in the weak-coupling regime, but is in the intermediate-coupling regime, with the precise nature of the supercurrent depending on the electronic state of the quantum dot.

There are also several types of tunnelling. Conventional tunnelling is a first-order process in which the initial and final states have the same energy. Co-tunnelling is a second-order process in which the particle tunnels from the initial state to a virtual state, and then to the final state. The initial and final states have the same energy in elastic co-tunnelling, but the virtual state can have any energy, although the probability of co-tunnelling decreases as the energy difference between the virtual and real states increases.

For a long time, all experiments were in the weak-coupling regime, with tunnelling occurring only through $1e$ quasiparticles. The first evidence for superconductivity in the transport properties of hybrid superconductor–quantum dot systems was reported for experiments on metallic grains in 1995¹¹. This work was performed in the weak-coupling regime and although there was no supercurrent transport, these experiments did provide clear signatures of the superconducting gap and the modified quasiparticle density of states near the gap. Technically it has been very difficult to increase the coupling for material reasons. For instance, oxidation of the interface between a superconductor and conventional semiconductors completely suppresses the tunnelling of Cooper pairs. Only

with the recent introduction of new materials, such as carbon nanotubes^{12–27}, semiconducting nanowires^{8,28–33}, self-assembled quantum dots^{9,34–36} and certain molecules¹⁰, have the regimes of intermediate and strong coupling become accessible.

Strongly coupled quantum dots

In the strong-coupling regime ($\Gamma \gg \Delta$ and $\Gamma \gg U$) the negligible charging energy U implies that the Coulomb blockade is absent, so it is equally likely that zero, one or two electrons (or holes) will be added to the quantum dot. This situation is similar to resonant tunnelling of non-interacting particles, except that the particles can be Cooper pairs as well as single electrons or holes. When superconductivity is suppressed (by applying a small magnetic field) we have the conventional resonant tunnelling^{2,3}; that is, conductance resonances with widths $\sim \Gamma$ are observed when $\epsilon_0 = 0$. We note that this normal-state conductance is dissipative. Typically a bias voltage is applied between the source and drain electrodes, and the resulting current is measured. Cooper-pair transport is measured as a supercurrent: a current is biased to increasing values, and the value where the voltage across the quantum dot becomes non-zero is recorded as the switching current⁷. The switching current (or experimentally maximum supercurrent) also shows resonant peaks whenever an orbital level is aligned with the condensate of Cooper pairs at the Fermi energy ϵ_F (Fig. 3a). In the case of spin-degenerate discrete levels in the quantum dot, the spacing in gate voltage between both types of resonant peak corresponds to adding two electrons to the lowest unoccupied discrete level and is proportional to the level spacing $\Delta\epsilon$.

The concept of resonant Cooper-pair tunnelling was originally proposed in 1982 by theorists who considered the possibility that impurities in a semiconductor weak link between two superconductors could provide a resonant path for Cooper pairs³⁷. Ten years later it was calculated³⁸ that the maximum value of the resonant supercurrent for a single non-interacting quantum dot between two superconductors with equal tunnel barriers would be $I_c = (\pi e/h)\Gamma\Delta/(\Delta + \Gamma/2)$. This simple expression for the critical

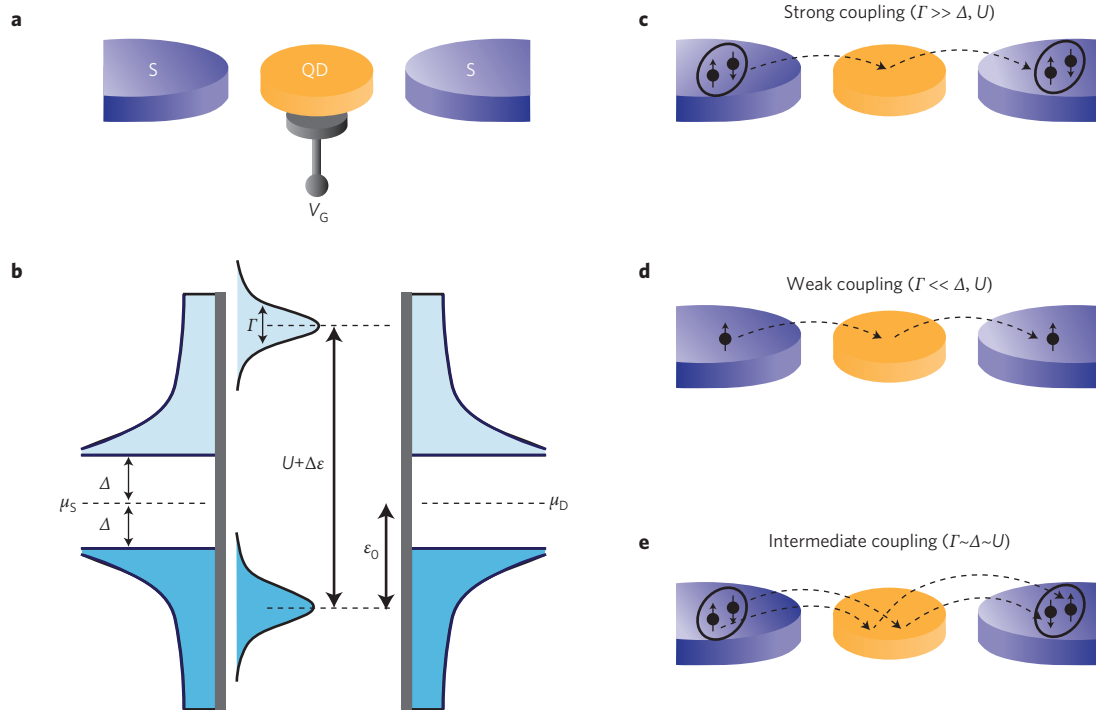


Figure 2 | Characteristic energy scales and transport regimes. **a**, Schematic device geometry with superconducting (S) source and drain electrodes attached to a generic quantum dot (QD) that is capacitively coupled to a gate electrode (V_G). **b**, Energy diagram for the device shown in **a**. Δ is the superconducting gap; μ_S and μ_D are the Fermi energies of the source and drain electrodes; Γ is the width of the quantum dot energy levels; U is the increase in electrostatic energy corresponding to the addition of a single electronic charge to the quantum dot; $\Delta\epsilon$ is the spacing between successive energy levels in the quantum dot; and ϵ_0 is the difference between the energy of the highest occupied level and the Fermi energy of the leads at zero bias (that is, $\epsilon_0 = \mu_S = \mu_D$). **c**, Supercurrents are the dominant transport mechanism in the strong-coupling regime: Cooper pairs can tunnel from the source to the drain through a single orbital level on the quantum dot when this level is aligned with the Fermi energies of the leads ($\epsilon_0 = 0$). **d**, Electron transport is only possible in the weak-coupling regime when single electrons can tunnel from filled quasiparticle states in the source to empty quasiparticle states in the drain. This requires a minimum applied bias voltage of $2\Delta/e$. **e**, In the intermediate-coupling regime, Cooper pairs can be transported from the source to the drain under certain conditions, with the phase shift (0 or π) depending on the electronic state of the quantum dot (see main text).

current holds for any Γ/Δ ratio if U can be neglected. In the limit $\Gamma \gg \Delta$, this expression reduces to $I_c = (\pi\Delta/e)G_0$, where $G_0 = 2e^2/h$ is the quantum of conductance. This result can be regarded as the supercurrent analogue of conductance quantization³⁹.

The strong-coupling limit was reached experimentally using single-walled carbon nanotubes as the quantum dots and Al-based superconducting electrodes^{16,19}. Nanotube quantum dots can have large energy-level spacing such that $\Delta\epsilon > \Gamma > \Delta > U$. Resonant supercurrent peaks were observed by varying a back-gate voltage (Fig. 3b). A comparison with the normal-state resonant conductance (for these parameters known as the Fabry–Perot regime⁴⁰) showed that the resonant supercurrent indeed occurs when the Fermi energy is aligned with a discrete quantum dot level and that the peak spacing corresponds to the addition of four electrons due to a two-fold orbital and a two-fold spin degeneracy.

However, the measured switching current was found to be an order of magnitude smaller than the theoretical critical current prediction, $I_c = (4\pi e/h)\Delta \sim 60$ nA (Fig. 3c). (The additional factor of 2 in this expression accounts for the two-fold orbital degeneracy in carbon nanotubes.) Part of this discrepancy is known to come from the electromagnetic environment of the junction, which includes the on-chip electrical circuit with various noise sources⁴¹. Later experiments^{20,23} used specially designed on-chip circuits to address these issues, but the theoretical predictions and the experimental results still differ by a factor of ~ 4 .

Weakly coupled quantum dots

In the weak-coupling regime ($\Gamma \ll \Delta$ and $\Gamma \ll U$) Cooper-pair tunnelling is largely suppressed, as explained above, but it is still possible

for single electrons to tunnel from occupied quasiparticle states in the source contact to empty states in the drain contact. For normal contacts, single-electron tunnelling occurs for arbitrarily small bias voltages provided a gate voltage is used to tune a quantum dot level so that it has the same energy as the occupied states in the source and the unoccupied states in the drain (Fig. 4a, left panel). However, this is not the case for superconducting contacts. Owing to the absence of quasiparticle states in the superconducting gap, a minimum voltage $eV = 2\Delta$ must be applied to align occupied quasiparticle states in the source with empty states in the drain (Fig. 4a, right panel). Moreover, owing to the divergence of the density of states at the superconducting gap edges¹, the onset of single-electron tunnelling is expected to yield a sharp rise in the current, followed by a region of negative differential resistance. (The flat density of states in normal contacts leads to much simpler step-like behaviour.)

A direct comparison between the onset of single-electron tunnelling for normal-type and superconducting contacts can be made with the aid of a small magnetic field, which is used to suppress superconductivity while leaving the quantum dot properties essentially unchanged (Fig. 4a). The characteristic current step observed for normal-type contacts (just above the critical field of the contacts) evolves into an asymmetric peak as the magnetic field is removed, leading to the development of superconducting gaps in the contacts. The weak-coupling regime has also been investigated with a gate-controlled quantum dot in an n-doped InP nanowire connected to Al-based electrodes: the gate voltage was used to vary the electrostatic potential of the quantum dot, enabling a direct measurement of the superconducting gap and providing clear evidence for single-electron tunnelling processes²⁸.

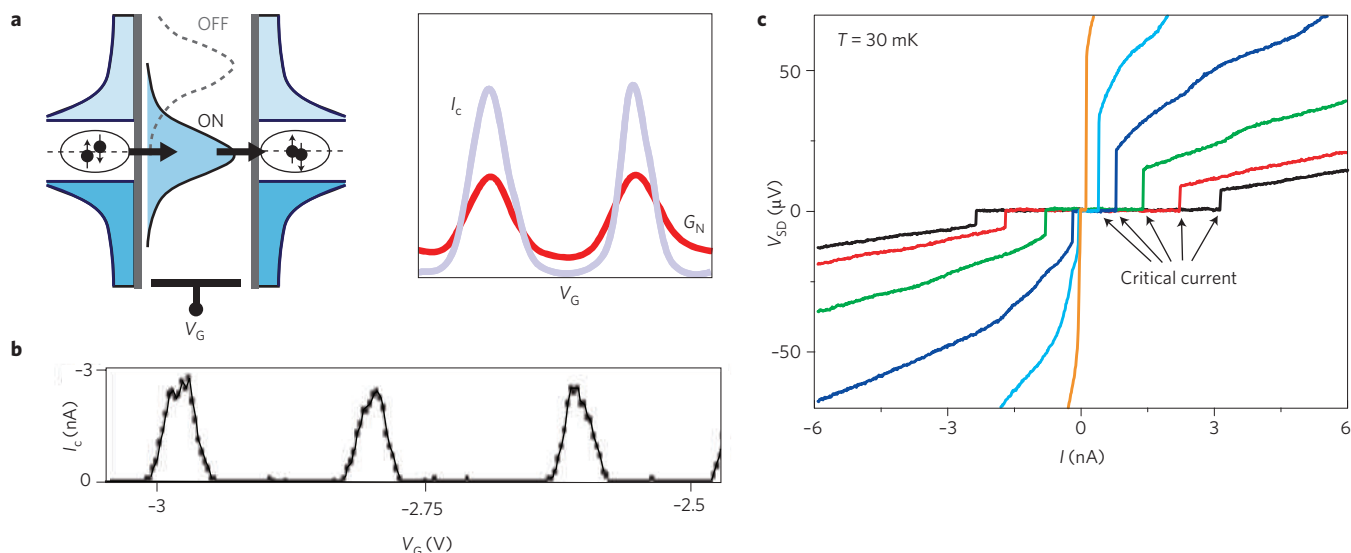


Figure 3 | Resonant Cooper-pair tunnelling in the strong-coupling regime. **a**, Energy level diagram showing how the quantum dot levels can be shifted in energy by a gate voltage V_G in the strong-coupling regime ($\Gamma \gg \Delta$; $\Gamma \gg U$). When a quantum dot level is aligned with the Fermi energy of the leads ($\epsilon_0 = 0$), a supercurrent can flow as a result of resonant Cooper-pair tunnelling ('ON' state). The corresponding critical current I_c is proportional to the resonance value of the normal-state conductance G_N . Away from resonance, when the Fermi energy lies between two consecutive dot levels, I_c is suppressed ('OFF' state). The right panel illustrates the device response in the superconducting (pale purple) and normal (red) state. On sweeping the gate voltage, the critical current and the normal-state conductance exhibit many resonance peaks corresponding to different quantum dot levels crossing the Fermi energy. When $\Gamma \gg \Delta$ we find that the Coulomb blockade has only a moderate impact on the electron transport properties at resonance: if we increase U so that $U \gg \Gamma \gg \Delta$, we find that the onset of a Coulomb blockade reduces the resonant values of I_c (which equals $2(\pi e/h)\Delta$ in theory) and G_N by only a small factor⁴³. However, the Coulomb blockade has a bigger impact as we approach the opposite limit. For $\Delta \gg \Gamma \gg U$ (that is, no Coulomb blockade), we find that the level broadening (which is small) suppresses the critical current by a factor of Γ/Δ to give $I_c \sim (\pi e/h)\Gamma$. However, for $U \gg \Gamma$ (blockade present) and $\Delta \gg \Gamma$, we find that the critical current is suppressed by the larger factor of $(\Gamma/\Delta)^2$ to give $I_c \sim (\pi e/h) \Gamma^2/\Delta$. **b**, The critical current I_c versus the gate voltage V_G for a carbon nanotube quantum dot connected to Ti/Al superconducting contacts¹⁶. Changing V_G shifts the energy levels in the nanotube and a peak in I_c is observed every time a nanotube level is aligned with the Fermi energy. **c**, Bias voltage V_{SD} versus current I for six different values of V_G between -2.590 V (black trace, ON state) and -2.541 V (orange trace, OFF state)¹⁶. For each value of V_G currents below a certain value (called the switching current) flow through the device without producing any voltage drop; when the current exceeds this value the device switches to a dissipative state with finite resistance and thus produces a voltage drop. The critical current I_c can be determined from the switching current. Measurements like this are used to provide the data for plots such as Fig. 3b. ($\Gamma \ll \Delta$ and $\Gamma \ll U$) ($\Gamma \sim \Delta \sim U$). Figures reproduced from: **b,c**, ref. 16, © 2006 NPG.

If U is not much larger than Γ , or at least if $\epsilon_0 \sim \Gamma$, a measurable quasiparticle current can result from second-order co-tunnelling processes. Each of these processes consists of two tunnelling events, which may be thought of as occurring one after the other⁴² (Fig. 4b). The first event takes an electron from the highest-occupied quantum dot level to an empty quasiparticle state in the drain contact, leaving the quantum dot in an intermediate virtual state. The second event takes an electron from an occupied state in the source contact to the initial quantum dot level. The net result of this process is to transfer a quasiparticle from the source to the drain without changing the state of the quantum dot. In the case of superconducting contacts, co-tunnelling processes require a bias voltage of at least $2\Delta/e$ to be applied to bring the occupied states in the source and the unoccupied states in the drain into resonance. Contrary to single-electron tunnelling, this threshold is independent of the gate voltage. Co-tunnelling features have been experimentally observed for different types of quantum dot^{8,9,24}. Figure 4c shows the differential conductance dI/dV , for a carbon nanotube quantum dot²⁴: the peaks at $V = \pm 2\Delta/e$ are owing to the divergence in the density of states mentioned above.

A second-order co-tunnelling process is required to transfer one quasiparticle from the source to the drain, whereas a fourth-order process is needed to transfer a Cooper pair. But is Cooper-pair transport possible in the presence of Coulomb blockade? And if it is, what kind of Josephson coupling can be expected? These questions are addressed in the next section where both conditions, $\Gamma \ll \Delta$ and $\Gamma \ll U$, will be simultaneously released.

Intermediately coupled quantum dots

In the intermediate-coupling regime all the energy scales are comparable ($\Gamma \sim \Delta \sim U$), which makes this the most complex regime — and also the most intriguing. The first condition, $\Gamma \sim \Delta$, can be sufficient to observe a sizable supercurrent, provided a quantum dot level can be aligned to the Fermi energy of the leads by a gate voltage. For large U , theorists have shown⁴³ that this resonant supercurrent is only a few times smaller than in the non-interacting case ($U = 0$). The second condition, $\Gamma \sim U$, ensures that a sizable supercurrent can still emerge when there is no quantum dot level aligned to the Fermi energy of the leads: this off-resonance supercurrent is carried by fourth-order co-tunnelling processes whose probability increases as Γ approaches U . Furthermore, the charging energy is large enough for the quantum dot to have, in the Coulomb blockade regime, reasonably well-defined spin and charge eigenstates. So in this regime the competition between quantum-coupled superconductors and trapped electrons is most apparent. In fact, the quantum dot states can give an extra phase to the quantum coupling between the superconductors, which can even reverse the direction of the supercurrent.

To understand this supercurrent reversal, one should consider the physical origin of a supercurrent. In a superconductor, Cooper pairs are condensed in a collective quantum state, which is characterized by a single, macroscopic quantum phase ϕ (the so-called superconducting order parameter). Normal-state currents are driven by voltage gradients, whereas non-dissipative supercurrents are driven by gradients in ϕ . Two weakly coupled superconductors can have different

φ , and in 1962 it was shown (by Josephson⁴) that this results in a supercurrent $I_s = I_c \sin(\Delta\varphi)$. This sinusoidal relation describes most superconducting junctions, but higher harmonics can also contribute to the current–phase relationship. There is also a second solution, $I_s = I_c \sin(\Delta\varphi + \pi) = -I_c \sin(\Delta\varphi)$, which is the same as the first solution except for the change of sign. (For both solutions I_s is zero when the phase difference $\Delta\varphi$ is zero, as is required by time-reversal symmetry.) This second solution defines a so-called π junction, and the change of sign in the critical current implies that, for a given phase difference, the supercurrent through a π junction is reversed with respect to an ordinary Josephson junction.

In 1977 it was predicted that magnetic impurities in the insulating layer could lead to a reversal of the critical current in a Josephson junction⁴⁴. It was also shown that the lowest energy state of a superconducting loop containing such a π junction can have a finite circulating supercurrent and a finite magnetic flux; in an ordinary junction the supercurrent and flux are always zero in the ground state. (This is related to the fact that the state with $I_s = 0$ and $\Delta\varphi = 0$ is stable in an ordinary junction, but is unstable in a π junction for which the energy minimum is at $\Delta\varphi = \pi$).

Following pioneering work⁴⁴, other types of π junction have been proposed and demonstrated experimentally^{45,46}, including Josephson junctions made from a ferromagnetic metal sandwiched between superconductors^{47,48}, SQUIDs that include a d -wave superconductor⁴⁹, and junctions formed by a normal metal with a non-thermal electron distribution⁵⁰. The physical origin of the π -phase shift differs for all these cases, being related to special symmetry

properties of the superconductors or to the tunnelling/conduction properties of the weak link.

The case of a quantum dot embedded inside a tunnel junction can be regarded as a version of the single-impurity limit in the π junctions originally proposed⁴⁴ and still not demonstrated experimentally. Figure 5a sketches an intuitive explanation for this type of π junction⁵¹: a Cooper pair crosses a quantum dot confining an even number of electrons in a spin-singlet state. Cooper pairs in conventional materials such as Al and Nb also form spin singlets. Each Cooper-pair transfer involves four processes: (1) spin- \downarrow tunnels out of the quantum dot creating a virtual quasiparticle excitation and leaving the quantum dot in a high-energy, virtual state; (2) a spin- \downarrow tunnels in, breaking up a Cooper pair in the left lead; (3) spin- \uparrow tunnels out, forming a Cooper pair on the right; (4) the remaining spin- \uparrow tunnels in from the left, bringing the quantum dot to its original ground state. This sequence of processes transfers a Cooper-pair singlet state from the left side, $|\psi\rangle_L = (|\uparrow\downarrow\rangle - |\downarrow\uparrow\rangle)$, to the right side, $|\psi\rangle_R = (|\uparrow\downarrow\rangle + |\downarrow\uparrow\rangle)$. (Note that we ignore normalization of the singlet state.) Because no phase change occurs during this transfer, one obtains the ordinary Josephson relation.

When the quantum dot is occupied by an odd number of electrons (forming a spin-doublet ground state), the sequence is: (1) spin- \uparrow tunnels out; (2) spin- \downarrow from a Cooper pair in the left lead tunnels in; (3) this same spin- \downarrow tunnels out and combines with the spin- \uparrow to form a Cooper pair on the right; (4) the remaining spin- \uparrow tunnels in from the left. The final spin on the quantum dot is the same as the initial spin. However, the spin ordering is reversed

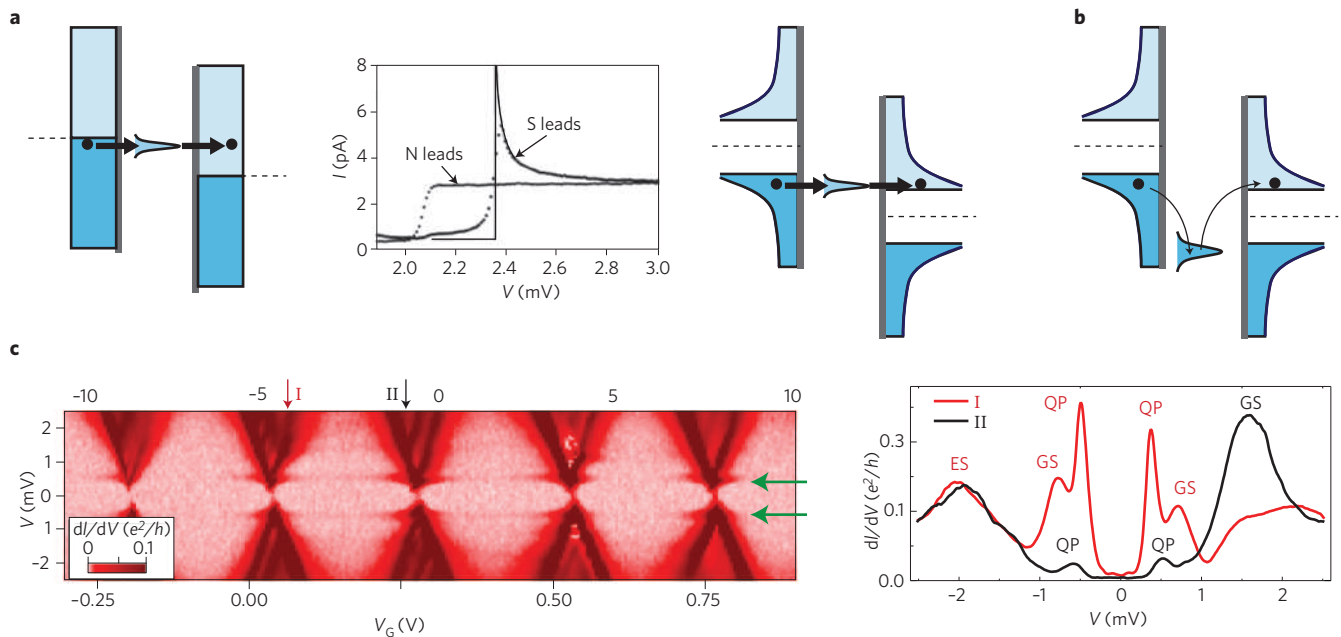


Figure 4 | Quasiparticle tunnelling in the weak-coupling regime. **a**, The tunnelling of Cooper pairs is suppressed in the weak-coupling regime ($\Gamma \ll \Delta$; $\Gamma \ll U$), and quasiparticle tunnelling is only possible if a quantum dot level is simultaneously aligned with occupied quasiparticle states in the source and empty quasiparticle states in the drain (right panel). This condition is fulfilled if $|V| > 2\Delta/e$, provided a gate voltage can be used to compensate for U and $\Delta\epsilon$. Without a gate, a further bias voltage of up to $(U + \Delta\epsilon)/e$ would be required, as is the case for normal-type electrodes (left panel). In the normal state (N leads) the onset of quasiparticle tunnelling leads to a step-like increase in the current, I , as the bias voltage, V , is increased; in the superconducting state (S leads) I first increases rapidly and then drops off slowly to approach the normal-state current level (middle panel). This negative differential resistance follows from the gap-edge singularities in the density of states of the superconducting leads: $I \sim eI/h$ and Γ is proportional to the density of states of the leads at the energy of the resonant level. **b**, Transfer of a quasiparticle by a second-order co-tunnelling process. **c**, Left panel: differential conductance, dI/dV , as a function of the bias voltage V and the gate voltage V_g for a carbon nanotube quantum dot connected to Nb-based superconducting electrodes. When Γ is smaller than U , but still of the same order as U , a measurable quasiparticle (QP) co-tunnelling current is observed within the Coulomb diamonds. The green arrows indicate the dI/dV peaks associated with the onset of elastic co-tunnelling at $|V| = \pm 2\Delta/e$. Right panel: selected traces showing dI/dV versus V . The extra dI/dV peaks correspond to the onset of sequential tunnelling through ground-state (GS) and excited-state (ES) levels. These peaks are not followed by negative dI/dV because of the relatively large life-time broadening of the quantum dot levels, so the gap-edge singularities emerge only in the co-tunnelling regime. Figures reproduced with permission from: **a** (middle panel), ref. 11, © 1995 APS; **c**, ref. 24, © 2009 APS.

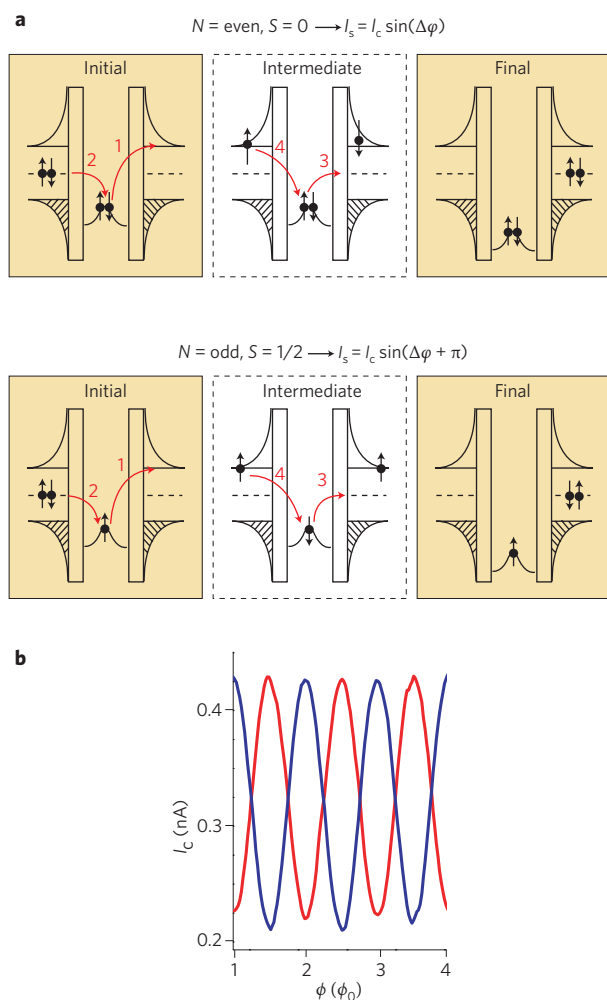


Figure 5 | Supercurrent reversal in the intermediate-coupling regime ($\Gamma \sim \Delta \sim U$). **a**, If Γ is not much smaller than U , co-tunnelling enables the coherent transfer of Cooper pairs across a quantum dot in the Coulomb blockade regime. For the simplest case of a single spin-degenerate level, the resulting Josephson coupling depends on its occupation. For a fully occupied (or empty) level and a total spin $S = 0$ on the dot, the fourth-order co-tunnelling process can be seen as a sequence of four tunnelling events labelled as 1, 2, 3 and 4. The order in which the spins of a Cooper pair are annihilated in the left lead is the same as the order in which they are created to form a Cooper pair in the right lead. This results in a usual current–phase relation. For a singly occupied level (or, more generically, an odd number N of confined electrons and a total spin $S = 1/2$), the spin ordering is reversed leading to a π phase shift in the current–phase relation. For a fixed phase difference $\Delta\varphi$ between left and right leads, changing the dot occupation by one electron causes the reversal of the supercurrent. **b**, Critical current I_c versus the magnetic flux ϕ through a SQUID with an embedded quantum dot at gate voltages corresponding to an even (blue) and odd (red) number of electrons on the quantum dot; ϕ is plotted in units of the flux quantum $\phi_0 = h/2e$. The phase difference of π between the two traces is clear. Reproduced from ref. 8, © 2006 NPG.

in the Cooper pair on the right side: $|\psi\rangle_R = (|\downarrow\uparrow\rangle - |\uparrow\downarrow\rangle) = e^{i\pi} |\psi\rangle_L$. The above sequence of tunnel processes is the only fourth-order process that transfers a Cooper pair across the quantum dot. The transfer amplitude thus picks up a π phase, which translates to a π -phase shift in the Josephson relation, that is, the critical current reverses.

The presence of a π -phase shift in the Josephson relation can be determined experimentally by embedding the quantum dot in

a SQUID device containing a second, reference junction with a known current–phase relationship. Such devices have been made with InAs nanowires⁸ (see Fig. 1a) and carbon nanotubes¹⁸ (Fig. 6a). In both cases, a π -phase shift was observed for an odd number of electrons on the quantum dot, whereas the phase shift was generally absent in the case of even occupation, in line with the schemes of Fig. 5a. Although the exact number of confined electrons was unknown in these experiments, the data revealed a clear even–odd asymmetry demonstrating that a supercurrent of $\sim 10^{-10} - 10^{-9}$ A (that is, billions of Cooper pairs per second) can be reversed simply by adding (removing) an electron to (from) the quantum dot. The π -phase shift associated with this sign change emerges clearly in the measurement of the SQUID switching current as a function of a perpendicular magnetic field. By varying a gate voltage, the occupancy of the quantum dot can be changed from even to odd, leading to a π jump in the phase of the SQUID oscillations (Fig. 5b).

When the tunnel coupling between the quantum dot and the contacts is strong enough, even higher-order co-tunnelling processes (that is, beyond the fourth order necessary to transfer a Cooper pair) become important. Indeed, for a quantum dot with an odd number of electrons and a spin-1/2 ground state, high-order co-tunnelling processes can screen the local spin moment through the formation of a many-body spin singlet state called a Kondo state. On average, the quantum dot spin gets bound to one electron from the leads with a characteristic binding energy $k_B T_K$, where k_B is the Boltzmann constant and T_K is the Kondo temperature⁵².

In the case of normal-type electrodes, the Kondo many-body state introduces a resonant level at the Fermi energy of the electrodes leading to an enhanced conductance. When $T \ll T_K$, the quantum dot conductance approaches $2e^2/h$ (for symmetric tunnel coupling), and Coulomb blockade is entirely lifted⁵³. As the electrodes become superconducting, the formation of the Kondo singlet competes with the tendency of the electrons around the Fermi energy to pair with each other. The resulting physics is governed by the ratio T_K/Δ . For $T_K/\Delta \ll 1$, the Kondo effect is suppressed and the quantum dot ground state is a spin doublet, and π -junction behaviour is thus expected as discussed before. In the opposite limit, $\Delta < T_K$, the Kondo effect wins and the singlet bound state at the Fermi energy provides a resonant tunnelling path for Cooper pairs resulting in a Josephson relation with no π -phase shift⁴³. The crossover between these two regimes underlies a quantum phase transition.

For more than 20 years, the competition between Kondo physics and superconductivity (including related phenomena such as multiple Andreev reflections) has been explored by theorists^{43,54–63}. The development of the superconductor–quantum dot systems described here is now stimulating experimental activity in this field^{14,18,21,23,24,30,31,34–36}.

Outlook

Classical Josephson junctions have been developed into a variety of devices, notably high-resolution sensors such as ultra-sensitive SQUID-based detectors for measuring magnetic flux. Superconducting photon detectors are now routinely used for applications in astronomy, and superconducting qubits based on Josephson junctions have also been demonstrated⁶. In most of these devices, the tunnel barrier between the two superconductors is an insulating dielectric, in many cases aluminium oxide. However, junctions in which the tunnel barrier is a normal metal have also been explored (in, for example, studies of Cooper-pair diffusion through disordered conductors), and the concept of Andreev reflection is often used to describe the conversion of normal state electrons into Cooper pairs in these devices. Very recently, Andreev bound states have been measured in a carbon nanotube⁶⁴ and in a graphene sample⁶⁵ connected to two superconductors.

In this Review we have, so far, focussed on devices in which the tunnel barrier is a quantum dot. Below we will conclude by

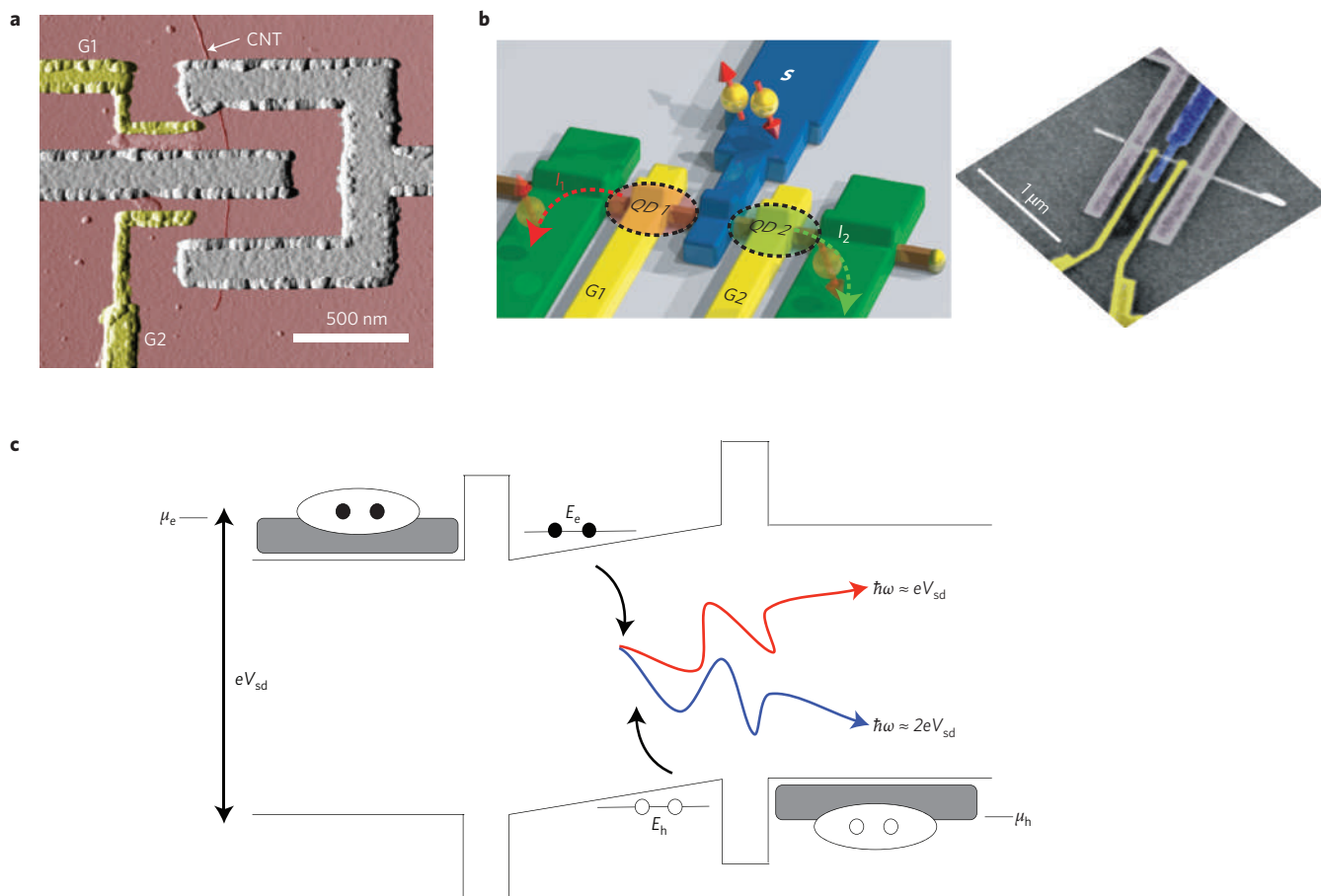


Figure 6 | Progress towards molecular spin detectors, spin entanglers, and Josephson light-emitting diodes. **a**, AFM image of a nanoSQUID device with the two Josephson junctions formed by distinct sections of the same carbon nanotube (CNT; red)¹⁸. The two gates (G1 and G2; yellow) allow the adjustment of the Josephson coupling in the respective junctions. This type of device could be used as a sensitive magnetometer to detect the magnetic moment of individual molecules positioned at the nanotube junction. **b**, Illustration of a Cooper-pair splitter (left panel). Electrons are paired in the superconducting electrode (S; shown in blue). The two quantum dots (QD 1 and QD 2; dotted circles) can hold only one electron each, so an incoming Cooper pair is split into two electrons, and the spatial separation of the electrons increases as they travel along the two outgoing leads (I_1 and I_2 ; green). This process has now been demonstrated in experiments in which the quantum dots were defined in a semiconductor nanowire⁷⁵ (SEM image in right panel) and in a carbon nanotube⁷⁶. The next challenge is to demonstrate the preservation of spin entanglement between the outgoing electrons. **c**, Energy level diagram for a proposed Josephson light-emitting diode: this device would consist of a superconducting electrode (not shown), heavily n-doped semiconductor (left), tunnel barrier, quantum dot, tunnel barrier, heavily p-doped semiconductor (right) and another superconducting electrode (not shown). Superconducting energy gaps are induced in the two heavily doped semiconductor regions by the proximity effect. The device is biased with a voltage V_{sd} such that the Cooper pairs in the conduction band on the left μ_e align with the electron state E_e in the quantum dot. Simultaneously, the Cooper pairs (of holes) in the valence band on the right μ_h align with the hole state E_h in the quantum dot. Electron-hole recombination results in the emission of photons at energy eV_{sd} and also at energy $2eV_{sd}$ as a direct result of the a.c. Josephson effect at optical frequencies. ω is frequency. Figures reproduced with permission from: **a**, ref. 18, © 2006 NPG; **b** (left panel), ref. 75, © 2009 NPG; **c**, ref. 78, © 2010 APS.

describing how hybrid superconductor–quantum dot devices are being developed for applications such as single-molecule SQUIDs, detectors for mechanical resonators and sources for entangled particles. We will also discuss the opportunities opened up by research at the interface between superconductivity and optics, and the possibility of detecting new types of particles in SQUID-based systems.

Single-molecule SQUIDs. The diameter of a carbon nanotube is approximately one nanometre. In Fig. 6a such a nanotube forms two Josephson junctions in a SQUID loop. The nanotube junctions provide an extreme spatial resolution that could be used for investigations of single magnetic molecules. Imagine a magnetic molecule placed close to the nanotube, just inside (or outside) the loop, so that the magnetic field lines from the molecule either add to (or subtract from) the flux through the SQUID. This extreme sensitivity is the motivation for developing such nanoSQUIDs for the detection of individual magnetic molecules^{18,66}.

Detectors for mechanical resonators. The extreme sensitivity to changes in enclosed flux has inspired another nanoscale application. Imagine the SQUID geometry in which the size of the loop can be altered, for instance when the junction has some mechanical degree of freedom. Such devices have been made by using freely suspended, nanomechanical oscillators as the junction, and resulting mechanical changes have been detected in the magnetic flux through the SQUID⁶⁷. The goal for these experiments is to be able to use changes in the critical current to measure the motion of extremely small mechanical resonators^{68–70}. Superconducting qubits based on conventional Josephson junctions (with insulators as tunnel barriers) have recently been used to control mechanical vibrations at the nanoscale in an experiment that cooled a micromechanical oscillator to its quantum ground state⁷¹.

Sources of entangled particles. Cooper pairs in conventional superconductors form singlet states. In general, the entanglement between

the electrons in a singlet state has the maximum possible value permitted by quantum theory (that is, they are maximally entangled Bell states), but these correlations are lost in a superconductor because all the Cooper pairs are mixed together in the condensate. However, the possibility of extracting a single Cooper pair from a superconductor to a quantum dot has inspired theoretical proposals to isolate and manipulate Cooper pairs such that the entanglement correlations can actually be measured^{72–74}. Experimenters have now responded to this challenge by coupling two quantum dots, each capable of holding one extra electron charge, to a superconducting lead (Fig. 6b). When a Cooper pair is extracted from the superconductor, it is forced to split into two (electron-like) particles, and these go to different quantum dots. Despite being separated in space, the two particles remain in their entangled singlet state, and they become further separated as they travel along the (normal-state) leads that are connected to the quantum dots^{75,76}.

The next challenge for experimentalists is to measure the correlations between the two particles as a function of their spatial separation. Such experiments will provide new insights into the quantum coherence of entangled electrons at a distance (the phase of a quantum state involving single or, as in this case, numerous particles tends to be randomized by its interactions with the host solid-state environment, a phenomenon that is generically known as decoherence). As well as shedding new light on fundamental aspects of quantum mechanics, this work could lead to new types of solid-state device that exploit quantum entanglement.

Interfaces between superconductors and optics. Superconductors are extremely sensitive to microwave signals because the energy of a typical microwave photon is comparable to a typical superconducting gap (a photon with a frequency of 100 GHz has an energy ~ 0.4 meV). Single Cooper-pair states can be converted into single microwave photons using qubit devices based on superconductor–insulator–superconductor junctions⁷⁷, but the coupling between superconductors and visible photons tends to be weak because these photons have energies that are about a thousand times larger than a typical superconducting gap. Recently it was proposed that the energy scales in the system, and hence the energies of the emitted photons, could be increased by including a pn junction in a superconductor–insulator–superconductor device⁷⁸ (Fig. 6c). Cooper pairs injected into both the n-doped and p-doped parts of the device can annihilate at the pn junction and emit the excess energy as visible photons. The inclusion of an optical quantum dot (that is, one that provides confinement for both electrons and holes) allows a controlled annihilation of individual Cooper pairs. Furthermore, the phase difference between the superconducting electrodes can be transferred to the emitted photons^{78,79}. Such a superconducting pn junction has never been realized, but if successful it would combine the advantages of fast superconducting electronics with long-distance coherence of photons.

Creation and manipulation of Majorana fermions. The discovery of antiparticles was an important breakthrough in the history of particle physics. The positron, for example, is the antiparticle of the electron, and these two particles are clearly different because they have opposite charges. However, it is also possible, in theory, for a neutral particle to be its own antiparticle, and such particles are known as Majorana fermions (as opposed to conventional Dirac fermions). Recently theorists have proposed that Majorana fermions could appear as the fundamental quasiparticles in systems in which superconductors are in contact with materials that have a strong spin–orbit interaction. These materials can be topological insulators (which have recently become the focus of intense research^{80–82}) or InAs nanowires^{83,84}. In this work, it is the one-dimensional subbands of the nanowires, rather than their quantum dot properties, that are important. The combination of one-dimensional subbands, strong spin–orbit interaction and induced superconductivity creates Andreev bound states at zero energy (that

is, bound to the Fermi energy), which have been shown to obey Majorana properties. The Majorana fermions could be detected with a SQUID-like geometry (such as the device in Fig. 1a) because they would cause the SQUID to oscillate with a period of 4π rather than the usual 2π periodicity^{83,84}.

The possibility of detecting a type of particle that has never been detected before indicates how far research into hybrid normal–superconductor nanodevices has progressed over the past decade. And even if Majorana fermions are not detected, there are good prospects for breakthroughs in other areas of physics and for the development of new types of device for a range of applications.

References

- Tinkham, M. *Introduction to Superconductivity* (McGraw-Hill, 1996).
- Kastner, M. A. Artificial atoms. *Phys. Today* **46**, 24–31 (January 1993).
- Kouwenhoven, L. P., Austing, D. G. & Tarucha, S. Few-electron quantum dots. *Rep. Prog. Phys.* **64**, 701–736 (2001).
- Josephson, B. D. Possible new effects in superconductive tunnelling. *Phys. Lett.* **1**, 251–253 (1962).
- Jaklevic, R. C. *et al.* Quantum interference effects in Josephson tunneling. *Phys. Rev. Lett.* **12**, 159–160 (1964).
- Clarke, J. & Wilhelm, F. K. Superconducting quantum bits. *Nature* **453**, 1031–1042 (2008).
- Likharev, K. K. Superconducting weak links. *Rev. Mod. Phys.* **51**, 101–159 (1979).
- van Dam, J. A., Nazarov, Y. V., Bakkers, E. P., De Franceschi, S. & Kouwenhoven, L. P. Supercurrent reversal in quantum dots. *Nature* **442**, 667–670 (2006).
- Katsaros, G. *et al.* Hybrid superconductor–semiconductor devices made from self-assembled SiGe nanocrystals on silicon. *Nature Nanotech.* **5**, 458–464 (2010).
- Winkelmann, C. B., Roch, N., Wernsdorfer, W., Bouchiat, V. & Balestro, F. Superconductivity in a single C_{60} transistor. *Nature Phys.* **5**, 876–879 (2009).
- Ralph, D. C., Black, C. T. & Tinkham, M. Spectroscopic measurements of discrete electronic states in single metal particles. *Phys. Rev. Lett.* **74**, 3241–3244 (1995).
- Kasumov, A. Y. *et al.* Supercurrents through single-walled carbon nanotubes. *Science* **284**, 1508–1511 (1999).
- Morpurgo, A. F., Kong, J., Marcus, C. M. & Dai, H. Gate-controlled superconducting proximity effect in carbon nanotubes. *Science* **286**, 263–265 (1999).
- Buitelaar, M. R., Nussbaumer, T. & Schönenberger, C. Quantum dot in the Kondo regime coupled to superconductors. *Phys. Rev. Lett.* **89**, 256801 (2002).
- Buitelaar, M. R. *et al.* Multiple Andreev reflections in a carbon nanotube quantum dot. *Phys. Rev. Lett.* **91**, 057005 (2003).
- Jarillo-Herrero, P., van Dam, J. A. & Kouwenhoven, L. P. Quantum supercurrent transistors in carbon nanotubes. *Nature* **439**, 953–956 (2006).
- Jorgensen, H. I., Grove-Rasmussen, K., Novotny, T., Flensberg, K. & Lindelof, P. E. Electron transport in single-wall carbon nanotube weak links in the Fabry-Perot regime. *Phys. Rev. Lett.* **96**, 207003 (2006).
- Cleuziou, J.-P., Wernsdorfer, W., Bouchiat, V., Ondarcuhu, T. & Monthieux, M. Carbon nanotube superconducting quantum interference device. *Nature Nanotech.* **1**, 53–59 (2006).
- Cleuziou, J.-P., Wernsdorfer, W., Bouchiat, V., Ondarcuhu, T. & Monthieux, M. Gate-tuned high frequency response of carbon nanotube Josephson junctions. *Phys. Rev. Lett.* **99**, 117001 (2007).
- Ingerslev Jørgensen, H. *et al.* Critical current $0-\pi$ transition in designed Josephson quantum dot junctions. *Nano Lett.* **7**, 2441–2445 (2007).
- Eichler, A. *et al.* Even-odd effect in Andreev transport through a carbon nanotube quantum dot. *Phys. Rev. Lett.* **99**, 126602–126605 (2007).
- Pallecchi, E., Gaass, M., Ryndyk, D. A. & Strunk, C. Carbon nanotube Josephson junctions with Nb contacts. *Appl. Phys. Lett.* **93**, 072501 (2008).
- Eichler, A. *et al.* Tuning the Josephson current in carbon nanotubes with the Kondo effect. *Phys. Rev. B* **79**, 161407 (2009).
- Grove-Rasmussen, K. *et al.* Superconductivity-enhanced bias spectroscopy in carbon nanotube quantum dots. *Phys. Rev. B* **79**, 134518 (2009).
- Jorgensen, H. I., Grove-Rasmussen, K., Flensberg, K. & Lindelof, P. E. Critical and excess current through an open quantum dot: Temperature and magnetic-field dependence. *Phys. Rev. B* **79**, 155441 (2009).
- Wu, F. *et al.* Single-walled carbon nanotube weak links in Kondo regime with zero-field splitting. *Phys. Rev. B* **79**, 073404 (2009).
- Liu, G., Zhang, Y. & Lau, C. N. Gate-tunable dissipation and “superconductor–insulator” transition in carbon nanotube Josephson junctions. *Phys. Rev. Lett.* **102**, 016803–016806 (2009).
- Doh, Y. J. *et al.* Tunable supercurrent through semiconductor nanowires. *Science* **309**, 272–275 (2005).

29. Xiang, J. *et al.* Ge/Si nanowire mesoscopic Josephson junctions. *Nature Nanotech.* **1**, 208–213 (2006).
30. Sand-Jespersen, T. *et al.* Kondo-enhanced Andreev tunneling in InAs nanowire quantum dots. *Phys. Rev. Lett.* **99**, 126603–126206 (2007).
31. Sand-Jespersen, T. *et al.* Tunable double dots and Kondo enhanced Andreev transport in InAs nanowires. *J. Vac. Sci. Technol. B* **26**, 1609–1612 (2008).
32. Doh, Y. J. *et al.* Andreev reflection versus Coulomb blockade in hybrid semiconductor nanowire devices. *Nano Lett.* **8**, 4098–4102 (2008).
33. Frielinghaus, R. *et al.* Josephson supercurrent in Nb/InN-nanowire/Nb junctions. *Appl. Phys. Lett.* **96**, 132504–132506 (2010).
34. Buijzert, C., Otiwa, A., Shibata, K., Hirakawa, K. & Tarucha, S. Kondo universal scaling for a quantum dot coupled to superconducting leads. *Phys. Rev. Lett.* **99**, 136806 (2007).
35. Deacon, R. S. *et al.* Tunneling spectroscopy of Andreev energy levels in a quantum dot coupled to a superconductor. *Phys. Rev. Lett.* **104**, 076805 (2010).
36. Kanai, Y. *et al.* Electrical control of Kondo effect and superconducting transport in a side-gated InAs quantum dot Josephson junction. Available at <http://arxiv.org/abs/0912.3094> (2009).
37. Aslamazov, A. G. & Fistul, M. V. Resonant tunneling in superconductor-semiconductor-superconductor junctions. *Sov. Phys. JETP* **55**, 681–684 (1982).
38. Beenakker, C. W. J. & van Houten, H. in *Single-Electron Tunneling and Mesoscopic Devices* (eds Koch, H. & Lübbig, H.) 175–179 (Springer, 1992); see also <http://xxx.lanl.gov/abs/condmat/0111505> (2001).
39. Beenakker, C. W. J. & van Houten, H. Josephson current through a superconducting quantum point contact shorter than the coherence length. *Phys. Rev. Lett.* **66**, 3056–3059 (1991).
40. Liang, W. J. *et al.* Fabry–Perot interference in a nanotube electron waveguide. *Nature* **411**, 665–669 (2001).
41. Vion, D., Götze, M., Joyez, P., Esteve, D. & Devoret, M. H. Thermal activation above a dissipation barrier: switching of a small Josephson junction. *Phys. Rev. Lett.* **77**, 3435–3438 (1996).
42. Averin, D. V. & Nazarov, Yu. V. in *Single Charge Tunneling: Coulomb Blockade Phenomena in Nanostructures* (eds Grabert, H. & Devoret, M. H.) 217–247 (Plenum and NATO Scientific Affairs Division, 1992).
43. Glazman, L. I. & Matveev, K. A. Resonant Josephson current through Kondo impurities in a tunnel barrier. *JETP Lett.* **49**, 659–662 (1989).
44. Bulaevskii, L. N., Kuzii, V. V. & Sobyanin, A. A. Superconducting system with weak coupling to the current in the ground state. *JETP Lett.* **25**, 290–294 (1977).
45. Tsuei, C. C. & Kirtley, J. R. Pairing symmetry in cuprate superconductors. *Rev. Mod. Phys.* **72**, 969–1016 (2000).
46. Golubov, A. A., Kupriyanov, M. Yu & Il'ichev, E. The current-phase relation in Josephson junctions. *Rev. Mod. Phys.* **76**, 411–469 (2004).
47. Ryazanov, V. V. *et al.* Coupling of two superconductors through a ferromagnet: evidence for a pi junction. *Phys. Rev. Lett.* **86**, 2427–2430 (2001).
48. Kontos, T. *et al.* Josephson junction through a thin ferromagnetic layer: Negative coupling. *Phys. Rev. Lett.* **89**, 137007 (2002).
49. Wollman, D. A. *et al.* Experimental determination of the superconducting pairing state in YBCO from the phase coherence of YBCO-Pb dc SQUIDS. *Phys. Rev. Lett.* **71**, 2134–2137 (1993).
50. Baselmans, J. J. A. *et al.* Reversing the direction of the supercurrent in a controllable Josephson junction. *Nature* **397**, 43–45 (1999).
51. Spivak, B. I. & Kivelson, S. A. Negative local superfluid densities: The difference between dirty superconductors and dirty Bose liquids. *Phys. Rev. B* **43**, 3740–3743 (1991).
52. Kouwenhoven, L. & Glazman, L. Revival of the Kondo effect. *Phys. World* **14**, 33–38 (January 2001).
53. van der Wiel, W. G. *et al.* The Kondo effect in the unitary limit. *Science* **289**, 2105–2108 (2000).
54. Clerk, A. A. & Ambegaokar, V. Loss of π -junction behavior in an interacting impurity Josephson junction. *Phys. Rev. B* **61**, 9109–9112 (2000).
55. Rozhkov, A. V., Arovas, D. P. & Guinea, F. Josephson coupling through a quantum dot. *Phys. Rev. B* **64**, 233301 (2001).
56. Vecino, E., Martín-Rodero, A. & Levy Yeyati, A. Josephson current through a correlated quantum level: Andreev states and pi junction behavior. *Phys. Rev. B* **68**, 035105 (2003).
57. Avishai, Y., Golub, A. & Zaikin, A. D. Superconductor-quantum dot-superconductor junction in the Kondo regime. *Phys. Rev. B* **67**, 041301 (2003).
58. Choi, M. S., Lee, M., Kang, K. & Belzig, W. Kondo effect and Josephson current through a quantum dot between two superconductors. *Phys. Rev. B* **70**, 020502 (2004).
59. Siano, F. & Egger, R. Josephson current through a nanoscale magnetic quantum dot. *Phys. Rev. Lett.* **93**, 047002 (2004).
60. Oguri, A., Tanaka, Y. & Hewson, A. C. Quantum phase transition in a minimal model for the Kondo effect in a Josephson junction. *J. Phys. Soc. Jpn* **73**, 2494–2504 (2004).
61. Sellier, G., Kopp, T., Kroha, J. & Barash, Y. S. π junction behavior and Andreev bound states in Kondo quantum dots with superconducting leads. *Phys. Rev. B* **72**, 174502 (2005).
62. Karrasch, C., Oguri, A. & Meden V. Josephson current through a single Anderson impurity coupled to BCS leads. *Phys. Rev. B* **77**, 024517 (2008).
63. Meng, T., Florens, S. & Simon, P. Self-consistent description of Andreev bound states in Josephson quantum dot devices. *Phys. Rev. B* **79**, 224521 (2009).
64. Pillet, D.-H. *et al.* Revealing the electronic structure of a carbon nanotube carrying a supercurrent. Available at <http://arxiv.org/abs/1005.0443> (2010).
65. Dirks, T. *et al.* Andreev bound state spectroscopy in a graphene quantum dot. Available at <http://arxiv.org/abs/1005.2749> (2010).
66. Bouchiat, V. Detection of magnetic moments using a nano-SQUID: limits of resolution and sensitivity in near-field SQUID magnetometry. *Supercond. Sci. Technol.* **22**, 064002 (2009).
67. Etaki, S. *et al.* Motion detection of a micromechanical resonator embedded in a d.c. SQUID. *Nature Phys.* **4**, 785–788 (2008).
68. Xue, F. *et al.* Controllable coupling between flux qubit and nanomechanical resonator by magnetic field. *New J. Phys.* **9**, 35 (2007).
69. Sonne, G., Shekhter, R. I., Gorelik, L. Y., Kulinich, S. I. & Jonson, M. Superconducting pumping of nanomechanical vibrations. *Phys. Rev. B* **78**, 144501 (2008).
70. Sonne, G., Peña-Aza, M. E., Gorelik, L. Y., Shekhter, R. I. & Jonson, M. Cooling of a suspended nanowire by an ac Josephson current flow. *Phys. Rev. Lett.* **104**, 226802 (2010).
71. O'Connell, A. D. *et al.* Quantum ground state and single-phonon control of a mechanical resonator. *Nature* **464**, 697–703 (2010).
72. Recher, P., Sukhorukov, E. V. & Loss, D. Andreev tunneling, Coulomb blockade, and resonant transport of nonlocal spin-entangled electrons. *Phys. Rev. B* **63**, 165314 (2001).
73. Lesovik, G. B., Martin, T. & Blatter, G. Electronic entanglement in the vicinity of a superconductor. *Eur. Phys. J. B* **24**, 287–290 (2001).
74. Bouchiat, V. *et al.* Single-walled carbon nanotube-superconductor entangler: noise correlations and Einstein–Podolsky–Rosen states. *Nanotechnol.* **14**, 77–85 (2003).
75. Hofstetter, L., Csonka, S., Nygard, J. & Schönenberger, C. Cooper pair splitter realized in a two-quantum-dot Y-junction. *Nature* **461**, 960–963 (2009).
76. Herrmann, L. G. *et al.* Carbon nanotubes as Cooper-pair beam splitters. *Phys. Rev. Lett.* **104**, 026801 (2010).
77. Schoelkopf, R. J. & Girvin, S. M. Wiring up quantum systems. *Nature* **451**, 664–669 (2008).
78. Recher, P., Nazarov, Y. V. & Kouwenhoven, L. P. Josephson light-emitting diode. *Phys. Rev. Lett.* **104**, 156802 (2010).
79. Hassler, F., Nazarov, Y. V. & Kouwenhoven, L. P. Quantum manipulation in a Josephson light-emitting diode. *Nanotechnol.* **21**, 274004 (2010).
80. Fu, L. & Kane, C. L. Superconducting proximity effect and Majorana fermions at the surface of a topological insulator. *Phys. Rev. Lett.* **100**, 096407 (2008).
81. Alicea, J. Majorana fermions in a tunable semiconductor device. *Phys. Rev. B* **81**, 125318 (2010).
82. Sau, J. D., Lutchyn, R. M., Tewary, S. & Das Sarma, S. Generic new platform for topological quantum computation using semiconductor heterostructures. *Phys. Rev. Lett.* **104**, 040502 (2010).
83. Lutchyn, R. M., Sau, J. D. & Das Sarma, S. Majorana fermions and topological phase transition in semiconductor/superconductor heterostructures. Available at <http://arxiv.org/abs/1002.4033> (2010).
84. Oreg, Y., Refael, G. & von Oppen, F. Helical liquids and Majorana bound states in quantum wires. Available at <http://arxiv.org/abs/1003.1145> (2010).
85. Roch, N., Florens, S., Bouchiat, V., Wernsdorfer, W. & Balestro, F. Quantum phase transition in a single-molecule quantum dot. *Nature* **453**, 633–638 (2008).

Acknowledgements

We thank M. Houzet, S. Frolov and L. Glazman for helpful discussions. S.D.F. acknowledges financial support from the Agence Nationale de la Recherche (ANR) through the ACCESS and COHESION projects. W.W. acknowledges financial support from the ANR (ANR-08-NANO-002) and the European Research Council through the MolNanoSpin project.

Additional information

The authors declare no competing financial interests.